

Clinical studies of biceps anisotropy, relaxation and nonlinearity with a medical device for ultrasonic imaging

Timofey Krit, Mariya Begicheva, Yuly Kamalov, and Valery Andreev

Citation: [Proc. Mtgs. Acoust.](#) **34**, 020004 (2018); doi: 10.1121/2.0000923

View online: <https://doi.org/10.1121/2.0000923>

View Table of Contents: <http://asa.scitation.org/toc/pma/34/1>

Published by the [Acoustical Society of America](#)

Articles you may be interested in

[A hybrid method to simulate elastic wave scattering of three-dimensional objects](#)

The Journal of the Acoustical Society of America **144**, EL268 (2018); 10.1121/1.5059332

[Ultrasound in air—Guidelines, applications, public exposures, and claims of attacks in Cuba and China](#)

The Journal of the Acoustical Society of America **144**, 2473 (2018); 10.1121/1.5063351

[Micro-bubbles cloud's spectroscopic nonlinear coefficient measurements towards its characterization](#)

Proceedings of Meetings on Acoustics **34**, 045039 (2018); 10.1121/2.0000917

[Theoretical and numerical studies of the streaming generated by a vortex beam](#)

Proceedings of Meetings on Acoustics **34**, 045040 (2018); 10.1121/2.0000918

[Cavitation inception pressure and bubble cloud formation by backscattering from bubble interfaces in HIFU](#)

Proceedings of Meetings on Acoustics **34**, 045041 (2018); 10.1121/2.0000919

[Evaluation of quadratic nonlinearity in tensile curve from ultrasonic linear and nonlinear measurements](#)

Proceedings of Meetings on Acoustics **34**, 045043 (2018); 10.1121/2.0000926



21st International Symposium on Nonlinear Acoustics



Santa Fe, New Mexico, USA

July 9-13, 2018, 50th Anniversary

Biomedical Acoustics: Paper S3-4

Clinical studies of biceps anisotropy, relaxation and nonlinearity with a medical device for ultrasonic imaging

Timofey Krit and Mariya Begicheva

Department of Acoustics, Faculty of Physics, Moscow State University, Moscow, 119991, RUSSIAN FEDERATION; timofey@acs366.phys.msu.ru; mariya.letowa@yandex.ru

Yuly Kamalov

The Russian National Research Center of Surgery named after B.V. Petrovsky, Moscow, RUSSIAN FEDERATION; kamalov53@yandex.ru

Valery Andreev

Department of Acoustics, Faculty of Physics, Moscow State University, Moscow, 119991, RUSSIAN FEDERATION; andreev@acs366.phys.msu.ru

We applied a commercial ultrasonic clinical diagnostic system for studies of human biceps. The investigated area was visualized in B-mode at a frequency of 8 MHz. We selected 1 cm and 2.5 cm depths for shear wave excitation. On these depths, the focused ultrasonic wave caused the acoustical radiation force. Due to nonlinear mechanism of excitation, a shear wave arose. The results we have obtained show that the biceps have the shear moduli of the order of 10 kPa. The loaded biceps demonstrated the nonlinear behavior better pronounced for the volunteer with smaller body mass index (BMI). As the load on the biceps increases, the shear modulus measured along the muscle fibers grows. The observed growth was stronger for the shear modulus of the short head. The shear modulus, measured in the direction across the fibers of the biceps, does not depend on the magnitude of the applied load and remains at the unloaded value. In 1 minute after load is removed the biceps tend to relax and its shear moduli turn their initial values.



1. INTRODUCTION

As the name of the biceps brachii muscle implies, it has two heads and is located on the arm. The muscle is commonly referred to as simply the biceps. Both heads attach on the scapula. The long head arises from the supraglenoid tubercle and runs over the head of the humerus and out of the joint capsule to descend through the intertubercular (bicipital) groove to join with the short head that has come from the coracoid process. Because tendons of both heads cross the shoulder joint anteriorly, the biceps assist in shoulder flexion. However, its main function is at the elbow¹. Functionality of the biceps is extremely important, since it determines the ability to flex the arm at the elbow joint, which, of course, is important in the day-to-day functioning of the body, and when applying special loads. Advances in the experimental study of viscoelastic properties of muscles² in recent years are associated with the emergence of methods of elastography based on the use of shear waves³.

Ultrasonic elastography is a new technology with many potential applications. It is highly effective in diagnostics due to its ability to recognize and qualify various pathologies of tissues. In this paper, the elastography method was used to evaluate the normal physiological parameters of the biceps brachii for further practical application of elastography in clinical studies.

Modern medical ultrasound is performed mainly using the echo-pulse approach and the brightness mode of display (B-mode)⁴. The basic principles of visualization in B-mode today are almost the same as several decades ago. The approach is to send small ultrasonic pulses from an ultrasonic probe into the body. Since ultrasonic waves penetrate into the tissues of the body with different acoustic impedances, some of them are reflected back to the probe (echoes), and some continue to penetrate deeper. Echoes resulting from the reflection of a series of consecutive pulses are processed and combined to generate an image. Thus, the ultrasonic probe works both as a transducer (generating sound waves), and as a receiver (recording sound waves). The ultrasonic pulse is actually quite short, but since it passes along a straight path, it is often called an ultrasonic beam. The direction of propagation of ultrasound along the line of the beam is called the axial direction, and the direction in the image plane perpendicular to the axial direction is called the lateral direction. Usually only a small part of the ultrasonic pulse is returned as a reflected echo after reaching the surface of the body tissue, and the rest of the pulse continues to propagate along the beam line to a greater depth in the tissue. Measurements in the B-mode give only qualitative ideas about the state of the tissue, and the result of these measurements is not always accurate. There are more accurate methods of non-invasive diagnosis, based on the fact that the presence of heterogeneities in the tissues and various pathological changes has a strong effect on their shear elasticity.

Shear waves cannot penetrate at all depths necessary for non-invasive medical diagnostics of biological tissues. Thus, longitudinal ultrasonic waves are used for excitation and detection of shear waves in the investigated region to which the shear waves cannot propagate from the surface. Acoustic pulse-wave elastography was particularly popular among the methods based on the excitation of the shear waves with the ultrasound. In this paper, the acoustical radiation force impulse (ARFI) method is used, which was implemented in clinical devices since early 2000s⁵. Quantitative estimation of shear wave velocity is realized on the basis of well-known algorithm of excitation and registration of shear wave in tissue⁶. ARFI imaging technology consists in mechanical excitation of tissue using short acoustic impulses (pushing pulses) in the region of interest chosen by the researcher⁷. The pushing pulses excite shear waves that propagate in the region of interest, perpendicular to the acoustic pushing pulse. Shear waves cause localized micron displacements of the tissue. The pushing pulse is several hundred cycles long and differs in voltage from the B-mode pulse consisting of a short number of cycles. At the same time, imaging waves are generated. These waves are less intensive than the push impulse (1:100). Wave detection is used to determine the position of the shear wave in the tissue at each time point. The moment of interaction between the shear waves and the imaging waves indicates the period of time elapsed between the generation of shear waves and their complete passage through the region of interest. Writing the shear wave front in several places and comparing these measurements with the current time, we can determine the value of the shear wave velocity. The harder the area inside the tissue, the greater the velocity of the shear wave that propagates through this area.

Currently, ARFI technology is successfully used for non-invasive medical diagnostics of liver, kidney and other viscera⁸. The tissues studied with the help of this technology usually possess isotropy of the shear modulus. As the result, the shear wave propagating in any direction has the same velocity, i.e. the wave velocity measured in such tissues has the same value in any direction. The values of the velocities differ only in regions of shear modulus inhomogeneity, which correspond to the areas of location of pathological changes in tissues. ARFI technology is implemented in several models of ultrasonic scanners capable of generating short-range acoustic radiation forces. The action of such forces on the tissue causes the localized small (1-10 μm) displacements inside the tissue. The response of the tissue to the acting radiation force is registered with conventional pulses that form the image in the B mode. Two-dimensional images of tissue displacement are created by repeating this process along several lines of the image. As a result of cross-correlation processing of images obtained in the B-mode, the tissue displacement is monitored at different times. Thus, the shear wave velocity in the tissue is determined.

2. WAVE PROPAGATION THROUGH THE ANISOTROPIC MEDIUM

The dynamics of anisotropic media, including elastic waves in such media, is described by a system of equations

$$\rho \frac{\partial^2 u_i}{\partial t^2} = \lambda_{iklm} \frac{\partial^2 u_m}{\partial x_k \partial x_l} \quad (1)$$

In this equation, U_i stands for the displacement vector of an element of a continuous elastic medium, λ_{iklm} is the 4th-rank tensor of the elastic moduli. Generally, the number of independent elastic moduli is 21. For structures with hexagonal symmetry, the number of independent elastic moduli is 5 (A, B, C, D, F)⁹:

$$\lambda_{xxxx} = \lambda_{yyyy} = A, \lambda_{xyxy} = B, \lambda_{xxyy} = A - 2B, \lambda_{xxzz} = \lambda_{yyzz} = C, \lambda_{xzxz} = \lambda_{yzzy} = D, \lambda_{zzzz} = F.$$

The tensor components are written in the Cartesian coordinate system. The z axis is directed along the muscle fiber (Fig. 1). The muscle mechanical properties are assumed to be invariant under rotation about this axis¹⁰.



Figure 1. The direction of the axes according to the fiber direction in the model.

We search for a solution of the system of differential equations (1), in the form of the monochromatic waves

$$u_i = u_{i0} \exp(-i\omega t + ik_l x_l) \quad (2)$$

with a constant amplitude u_{i0} . The substitution of the form (2) in (1) results in

$$\rho \omega^2 u_i = \lambda_{iklm} k_k k_l u_m.$$

Considering $u_i = \delta_{im} u_m$ we can transform the previous expression into the system of equations

$$\left(\rho\omega^2\delta_{im} - \lambda_{iklm}k_k k_l\right)u_m = 0 \quad (3)$$

of three variables u_x, u_y, u_z . System (3) has non-zero solutions only when its determinant turns to zero:

$$\det\left\|\rho\omega^2\delta_{im} - \lambda_{iklm}k_k k_l\right\| = 0 \quad (4)$$

This equation determines the dependence of the frequency of the wave on the wave vector; it is called the dispersion relation. The solutions of the dispersion relation (4) are three frequency-independent wave velocities.

We choose the coordinate system so that the wave vector \vec{k} belongs to the xz plane. Thus, $k_x = k \sin \theta$, $k_y = 0$, $k_z = k \cos \theta$, where θ is the angle between the vector \vec{k} and axis z . Then the solutions of equation (4) are as follows

$$\rho\omega_1^2 = k^2 (B \sin^2 \theta + D \cos^2 \theta),$$

$$\rho\omega_{2,3}^2 = \frac{1}{2}k^2 \left\{ A \sin^2 \theta + F \cos^2 \theta + D \pm \left[((A-D) \sin^2 \theta + (F-D) \cos^2 \theta)^2 + 4(C+D)^2 \sin^2 \theta \cos^2 \theta \right]^{\frac{1}{2}} \right\}$$

In this work, when measurements were conducted, the shear wave polarization was not taken into account, since it was believed that there are only two directions of propagation: $\theta = 0$ and $\theta = 90^\circ$.

When the wave vector is directed along the z axis (the wave propagates along the muscle fibers, $\theta = 0$), one of the equation roots corresponds to the longitudinal wave, the other two roots are the same and refer to transverse waves:

$$c_l^2 = \frac{F}{\rho}, \quad c_{t_1}^2 = c_{t_2}^2 = \frac{D}{\rho}.$$

In case the wave vector is directed along the x axis (the wave propagates across the muscle fibers, $\theta = 90^\circ$), then all velocities are different:

$$c_l^2 = \frac{A}{\rho}, \quad c_{t_1}^2 = \frac{B}{\rho}, \quad c_{t_2}^2 = \frac{D}{\rho}.$$

That is the difference between the anisotropic medium and the isotropic one. The only longitudinal wave and two shear waves exist in an isotropic medium, and the velocities of the shear waves would coincide.

In the general case, for an arbitrary inclination of the wave vector to the z axis, it is not possible to separate the longitudinal and transverse waves.

However, the anisotropic properties of the medium change radically when the propagation velocities of longitudinal waves significantly exceed the shear wave velocities. Such media, in which shear elastic moduli are much smaller than those associated with the compressibility of the material, are called soft solids. An example of such a medium is muscle tissue.

It is shown in¹¹ that in the "soft solids" that the modules A, C, F have to be of the same order as ρc_l^2 , and the other two modules B, D have to be much smaller and to be of the same order as ρc_t^2 . Since the shear wave velocity in the muscle is 2 orders of magnitude smaller than the velocity of the longitudinal wave, this condition is obviously satisfied.

Then the velocities will be expressed as follows:

$$c_l^2 = \frac{A}{\rho}, c_{t_1}^2 = \frac{B}{\rho} \sin^2 \theta + \frac{D}{\rho} \cos^2 \theta, c_{t_2}^2 = \frac{D}{\rho}.$$

This means three waves can propagate in the muscle tissues: one longitudinal and two transverse. The speed of the first transverse wave is independent of the direction (this is a wave propagating along the fibers), and the speed of the second transverse wave depends on the direction (this is a wave propagating across the muscle fibers).

3. CLINICAL STUDIES OF THE LOADED BICEPS

The study was conducted in the laboratory of ultrasound diagnostics of the Russian National Research Center of Surgery named after B.V. Petrovsky by a doctor with experience in use of ultrasound diagnostic equipment. The volunteers were chosen among the employees and students of the Faculty of Physics of Moscow State University. All the volunteers were healthy without muscle injuries. The ultrasound diagnostic system of the expert level Siemens ACUSON S2000 was used with a standard diagnostic probe.

The strained condition of the biceps arm muscle was achieved by applying various loads. The method for creating the load was the following. We took special weight plates commonly used for barbells or dumbbells by the lifters. Four plates each of 1 kg and one plate of 5 kg were used. The combination of these plates, made it possible to form loads of 1, 2, 3, 4 and 5 kg. Each load created a strained state in the biceps muscle of the volunteer.

Before the measurements, each volunteer was at rest for 10-15 minutes, so that no physical activity, even potential, could affect the results. The initial position of the volunteer was the following: sitting on the couch opposite the doctor, the arm was bent at the elbow joint and had a rigid support under the elbow joint. The angle between the bones of the shoulder and forearm was 90°. In this case, both forearm and shoulder were located in a plane perpendicular to the support plane and both at an angle of 45° to the support. The volunteer's wrist was parallel to the support and the palm was up. Further, the biceps were loaded with the weight plates. The plates were stacked on the palm forming a pile¹². The average value of shear wave velocity in the biceps was obtained for various configurations: an unloaded muscle, a muscle loaded from 1 to 5 kg, and the muscle 1 min after removal of each load. The probe was applied directly to the skin and held by the doctor who carried out the measurements. In each configuration, measurements were taken in the short and long head of the muscle. The probe was positioned along and across the muscle fibers both in the short and long head.

The ARFI mode, available in the ACUSON S2000 system, is implemented as a Virtual Touch™ function. This function allows obtaining sonoelastograms, similar to those that can be obtained with conventional sonoelastography. This mode is used to characterize and visualize damage in tissues. Representative elastograms are presented in Fig. 2.

We introduce the effective shear modulus and we estimate it in the tissue area under study using the simple expression^{13, 14}:

$$\mu = \rho v^2, \quad (5)$$

where v is the velocity measured at certain position of the ultrasound probe, ρ is the average density.

The relevant protocol was prepared for the study. The first section of the protocol contains the questionnaire data of the subject. This section includes surname, name, patronymic, height and weight. The second section contains the recorded values of the shear wave velocities measured by the ARFI method at different loads at a depth corresponding to the middle of the short head of the biceps muscle. The depth is fixed for each subject and then does not change when the load changes. A series of three measurements was carried out with each load. Then the results of the measurements were averaged.

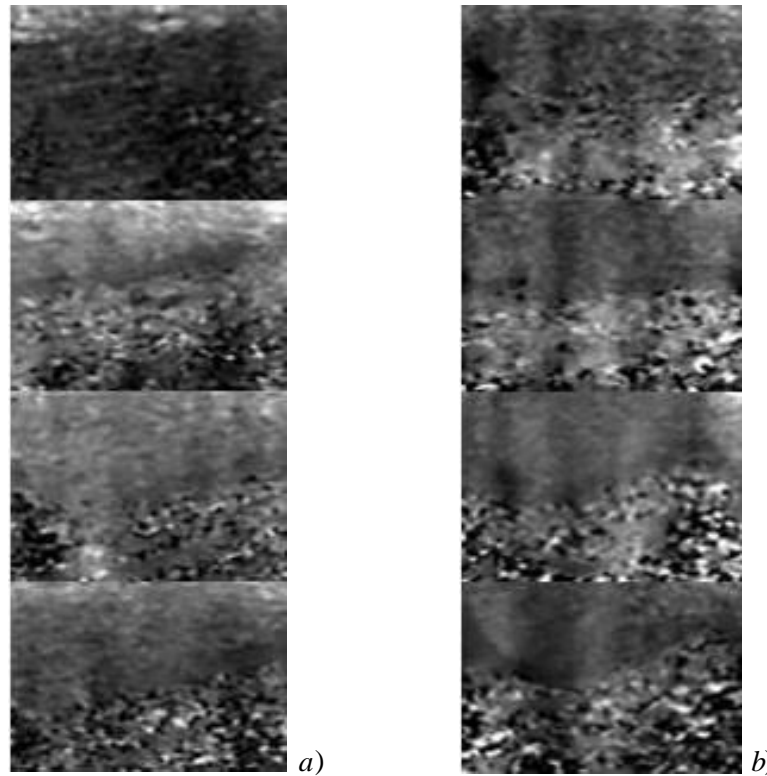


Figure 2. *Elastograms at the loads of 0, 1, 2, and 3 kg (top down) along (a) the muscle fibers and across (b) the muscle fibers.*

The shear wave velocities measured by the ARFI method at different loads at the depth corresponding to the middle of the long head of the biceps muscle were recorded in the third section of the protocol. The depth also was not changed when the load was varied. A series of three measurements was carried out with each load. The obtained results then were averaged. The fourth section of the protocol, like the second, was assigned for the values of shear wave velocities at a depth, which corresponded to the middle of the short head of the biceps. The measurements here, however, were conducted 1 minute after the load was removed. Similarly, in the fifth section of the protocol, as in the third section, the recorded shear wave velocities were measured by the ARFI method at a depth corresponding to the middle of the long head of the biceps muscle, but the measurements were conducted 1 minute after removal of each load.

As mentioned above, the anisotropy of the biceps arm muscle causes the difference in values of the shear wave velocities measured in the biceps along or across the muscle fibers. For this reason, the second, third, fourth and fifth sections of the protocol contain two subsections. The first subsection of each section contains the records of the velocities measured along the muscle fibers, i.e. when the direction of the fibers coincides with the long side of the probe. We call this probe position longitudinal. The second subsection of each section contains the records of the velocities measured across the muscle fibers, i.e. when the direction of the fibers is perpendicular to the long side of the probe. This position is mentioned below as a transverse.

4. MEASURED VALUES OF THE SHEAR MODULUS IN A BICEPS

Based on the measurement results, the shear modulus was plotted against the force applied to the muscle. The force was calculated by multiplying the load mass by the gravitational acceleration.

Fig. 3 shows the dependences of the shear moduli on the loads applied to the biceps measured for one of the volunteers. The examined volunteer was a man at the age of 31 years. His height was 174 cm, weight was 85 kg. The body mass index calculated from the questionnaire was 28.08. The unfilled rhombs show the results obtained at a depth of 1 cm with the longitudinal position of the probe. The filled triangles show the values of the shear moduli determined at a depth of 2.5 cm also for the longitudinal position of the probe. The results of measurements with transverse position of the probe at depths of 1 cm and 2.5 cm are shown with circles and crosses, respectively. The filled squares show the results of measuring the shear modulus along the muscle fibers at a depth of 1 cm in 1 min after removal of the corresponding load. The unfilled triangles show the results of measuring the shear modulus along the muscle fibers at a depth of 2.5 cm in 1 min after removal of the corresponding load. The presented data shows that the muscle gradually returns to its original state.

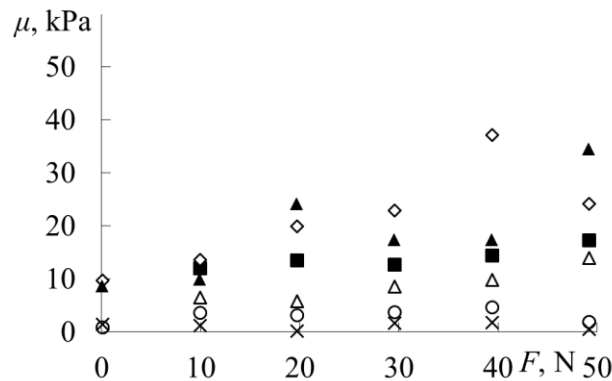


Figure 3. Measured shear modulus against the load applied to the volunteer's biceps.
Volunteer's profile: man, 31 y.o., BMI 28.08.

Similar measurements were made in the biceps muscle of a second volunteer with a smaller body mass index. The results of these measurements are shown in Fig. 4. The symbols on the graph were chosen similarly to Fig. 3. The dependence shows that the applied loads make the shear modulus measured in the short head with the longitudinal position of the probe increase first. After that sharp

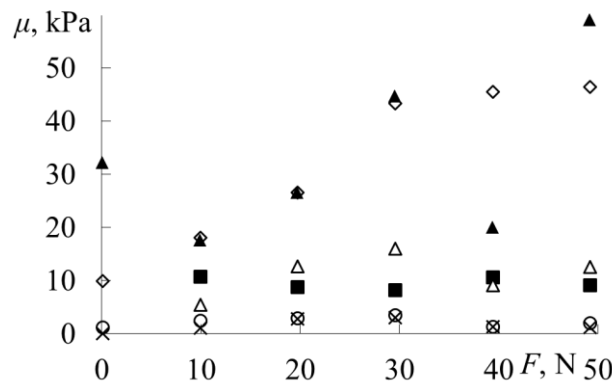


Figure 4. Measured shear modulus against the load applied to the volunteer's biceps.
Volunteer's profile: woman, 22 y.o., BMI 14.69.

increase, at loads above 30 N, the shear modulus reaches a constant level. The value of the shear modulus measured in the long head with the longitudinal position of the probe, at the loads up to 30 N, repeats the result for the short head. The further increase of the load results in a wide scatter of the measured values. Therefore, for the third volunteer (Fig. 5), we did not carry out the measurements at high loads. The measured results for the transverse position of the probe for all volunteers at different loads appeared to be the same within the error. The body mass index of the third and first volunteers is close, which led to similar measurement results.

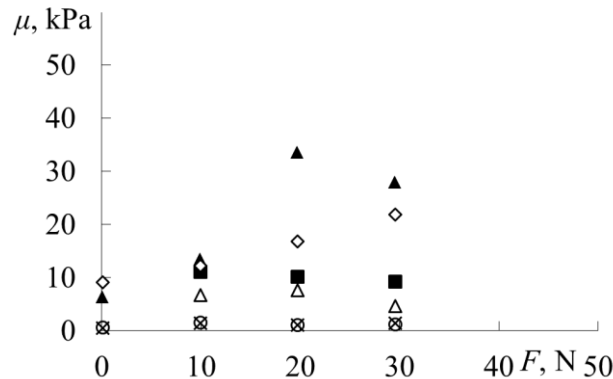


Figure 5. Measured shear modulus against the load applied to the volunteer's biceps.
Volunteer's profile: man, 22 y.o., BMI 25.06.

The results for the loads higher than 30 N were not recorded. The algorithm used in the clinical device to calculate the shear wave velocity has returned X signs instead of the values.

5. CONCLUSION

The results we have obtained show that the biceps have the shear moduli of the order of 10 kPa. The loaded biceps demonstrated the nonlinear behavior. This result is in a good agreement with the fact that the shear modulus of the soft tissues is dependent on the force applied to the tissues and the dependence can be described with the square polynomial¹⁵. The exact values found from the RMS analysis of the experimental results for the loaded biceps are summarized in Table 1. The RMS has shown that the square parabola perfectly fits the experimental results with the constants listed below.

Table 1. The shear constants obtained during the RMS analyzes of the loaded biceps behavior.

Depth, cm	1			2.5		
BMI	28.08	14.09	25.06	28.08	14.09	25.06
μ_0 , kPa	10.03	10.55	9.28	9.79	10.39	5.96
κ_1 , kPa/N	0.42	0.45	0.29	0.22	0.36	0.85
κ_2 , kPa/N ²	0.001	0.02	0.005	0.004	0.03	0.008

Here μ_0 stands for linear shear modulus, i.e. the absolute term. The linear term is denoted as κ_1 and the square one as κ_2 .

As the load on the muscle increases, the shear modulus measured along the muscle fibers of each of its heads grows, and the growth is stronger for the shear modulus of the short head. The shear modulus, measured in the direction across the muscle fibers, does not depend on the magnitude of the applied load and remains at the unloaded value. At the loads above 30 N, the values measured for the short and the long heads vary drastically. The reason was that the position of the volunteer was not secure

under high loads. Due to this fact the data obtained at the loads more than 30 N was not taken into account in the data evaluation processes. The increase we obtained for the longitudinal position of the probe shows the nonlinear behavior of the shear modulus of the biceps under the growing load. The result was better pronounced for the volunteer with smaller BMI. As the BMI grows up, the biceps tends to work more linearly. The methodology we suggest in this paper is clinically applicable, and in the future it will allow development of muscle elastography and precise diagnostics of muscle tissue pathologies in humans with various neuromuscular and muscular diseases.

ACKNOWLEDGMENTS

The reported study was funded by RFBR according to the research project № 16-02-00719 a.

REFERENCES

- ¹ Lippert L.S., Clinical kinesiology and anatomy, 4th ed. F. A. Davis Company, Philadelphia (2006)
- ² Gennisson J.-L., Deffieux T., Macé E., Montaldo G., Fink M., Tanter M., “Viscoelastic and anisotropic mechanical properties of in vivo muscle tissue assessed by supersonic shear imaging,” *Ultrasound Med. Biol.* **36**(5), 789–801 (2010).
- ³ Sarvazyan A.P., Rudenko O.V., Nyborg W.L., “Biomedical applications of radiation force of ultrasound: historical roots and physical basis,” *Ultrasound Med. Biol.* **36**(9), 1379–1389 (2010).
- ⁴ Diagnostic ultrasound: physics and equipment / [ed. by] Hoskins P., Martin K., Thrush A. – 2nd ed. Cambridge University Press (2010).
- ⁵ Nightingale K., Bentley R., Trahey G., “Observations of tissue response to acoustic radiation force: opportunities for imaging,” *Ultrason. Imag.* **24**(3), 129–138 (2002).
- ⁶ Andreev V.G., Dmitriev V.N., Pischalnikov Y.A., Rudenko O.V., Sapozhnikov O.A., Sarvazyan A.P., “Observation of shear waves excited by focused ultrasound in rubber-like medium,” *Acoust. Phys.* **43**(2), 123–128 (1997).
- ⁷ Lupsor M., Badea R., Stefanescu H., Sparchez Z., Branda H., Serban A., Maniu A., “Performance of a new elastographic method (ARFI technology) compared to unidimensional transient elastography in the noninvasive assessment of chronic hepatitis C. Preliminary results,” *J. Gastrointest. Liver Dis.* **18**(3), 303–310 (2009).
- ⁸ Nightingale K., “Acoustic Radiation Force Impulse (ARFI) Imaging: a Review,” *Curr. Med. Imaging Rev.* **7**(4), 328–339 (2011).
- ⁹ Landau L.D. and Lifshitz E.M. *Theory of Elasticity*, 3rd ed. Butterworth-Heinemann, Oxford (1986).
- ¹⁰ Wang M., Byram B., Palmeri M., Rouze N., Nightingale K., “Imaging transverse isotropic properties of muscle by monitoring acoustic radiation force induced shear waves using a 2D matrix ultrasound array,” *Trans Med Imaging.* **32**(9), 1671–1684 (2013).
- ¹¹ Rudenko O.V., Sarvazyan A.P., “Wave biomechanics of the skeletal muscle,” *Acoust. Phys.* **52**(6), 720–732 (2006).
- ¹² Yavuz A., Bora A., Bulut M.D., Batur A., Milanlioglu A., Goya C., Andic C., “Acoustic radiation force impulse (ARFI) elastography quantification of muscle stiffness over a course of gradual isometric contractions: a preliminary study,” *Med. Ultrason.* **17**(1), 49–57 (2015).
- ¹³ Andreev V.G., Krit T.B., Sapozhnikov O.A., “Standing waves in an elastic layer loaded with a finite mass,” *Acoust. Phys.* **56**(2), 168–173 (2010).
- ¹⁴ Rudenko O.V., Sarvazyan A.P., “Wave anisotropy of shear viscosity and elasticity,” *Acoust. Phys.* **60**(6), 710–718 (2014).
- ¹⁵ Abiza Z., Destrade M., Ogden R.W., “Large acoustoelastic effect,” *Wave Motion.* **49**(2), 364–374 (2012).